Electronic Supplementary Material (ESI) for Journal of Materials Chemistry A.
This journal is © The Royal Society of Chemistry 2021

Supplementary Information

Efficient, Thermally Stable Poly(3-Hexylthiophene)-Based Organic Solar Cells Achieved by Non-Covalently Fused-Ring Small Molecule Acceptors

Daehee Han, [a,†] *Yunghee Han,* [a,†] *Youngkwon Kim,* [a] *Jin-Woo Lee,* [a] *Dahyun Jeong,* [a] *Hyeonjung Park,* [a] *Geon-U Kim,* [a] *Felix Sunjoo Kim,* [c] *and Bumjoon J. Kim* [a, b*]

[a] Department of Chemical and Biomolecular Engineering and [b]KAIST Institute for the Nanocentury, Korea Advanced Institute of Science and Technology (KAIST), Daejeon 34141, Republic of Korea

[c] School of Chemical Engineering and Material Science Chung-Ang University (CAU), Seoul 06974, Republic of Korea

[*](B. J. Kim) E-mail: bumjoonkim@kaist.ac.kr

Table of Contents

Methods

Charaterizations

^{1}H nuclear magnetic resonance (NMR) spectra were recorded using a Bruker Avance 300 MHz spectrometer. Bruker Autoflex matrix-assisted laser desorption ionization-time of flight (MALDI-ToF) mass spectrometry was used for analysis mass of synthesized materials. UV-visible absorption spectra were measured with a UV-1800 spectrophotometer of Shimadzu Scientific Instruments. Cyclic voltammograms (CV) were measured using convenstional three-electrode with a VSP Potentiostat from BioLogic and EC-Lab software. The cyclic voltammetry measurements were conducted in anhydrous acetonitrile containing 0.1 M tetrabutylammonium hexafluorophosphate and calibrated against a ferrocene/ferrocenium (Fc/Fc^+) redox couple (potential scan rate: 50 mV s^{-1}), assuming that the absolute energy level of Fc/Fc^+ was -4.80 eV with respect to zero vacuum level.[1] Optical microscopy (OM) images were obtained using Nikon L150 OM in reflection mode under ambient conditions. Atomic force microscopy (AFM) height images were obtained using SmartScan of Park SYSTEMS NX10 in non-contact mode under ambient conditions. Transmission electron microscopy (TEM) images were acquired using JEOL 2000 FX. Grazing incidence X-ray scattering (GIXS) profiles were measured at the 9A beamline in the Pohang Accelerator Laboratory, Republic of Korea. The incidence angle of GIXS was 0.12° to allow for complete penetration the full height of thin films. Resonant soft X-ray scattering (RSoXS) profiles were measured at 11.0.1.2 beamline in the Advanced Light Source, United States. Differential scanning calorimetry (DSC) (TA Instruments) measurements were used to evaluate the thermal properties of CPDT-ICMe.

Fabrication of organic solar cells (OSCs)

The conventional structure OSCs, indium tin oxide (ITO)/poly(3,4-

ethylenedioxythiophene):polystyrene sulfonic acid (PEDOT:PSS, AI4083 from Heraeus)/active layer/polymer interlayer/Ag or Ca/Al) were fabricated by the following processes. Poly[[2,7-bis(2-ethylhexyl)-1,2,3,6,7,8-hexahydro-1,3,6,8-tetraoxobenzo[lmn][3,8]phenanthroline-4,9-diyl]-2,5-thiophenediyl[9,9-bis[3'((N,N-dimethyl)-N-ethylammonium)]-propyl]-9H-fluorene-2,7-diyl]-2,5-thiophenediyl] (PNDIT-F3N-Br) was used as polymer interlayer. ITO-coated glass substrates were treated with ultrasonication by acetone and isopropyl alcohol solvents. The cleaned substrates were dried for more than 1 hr at 80 °C in an oven, followed by plasma treatment for 10 min. The PEDOT:PSS solution was spin-casted at 3000 rpm for 30 sec and then thermally annealed at 165 °C for 15 min in ambient conditions. Then, the samples were moved into a N_2-filled glovebox. Next, the P3HT:acceptor blend solutions with optimal concentrations (16 mg mL^{-1} for both CPDT-ICMe and ZY-4Cl, and 25 mg mL^{-1} for $PC_{61}BM$) and D:A ratios (1:1 for CPDT-ICMe, 1:1.2 for ZY-4Cl, and 1:0.8 for $PC_{61}BM$) were prepared in tetrahydrofuran (CPDT-ICMe and ZY-4Cl) and chlorobenzene ($PC_{61}BM$). The solutions were stirred for at least 1 hr at 60 °C (CPDT-ICMe, ZY-4Cl) and 80 °C ($PC_{61}BM$) before spin-coating. Then, the solution was spin-cast onto the PEDOT:PSS-coated ITO substrates at 3000 rpm for 30 sec, and the films were thermally annealed at 130 °C for 5 min (CPDT-ICMe, ZY-4Cl) and 150 °C for 10 min ($PC_{61}BM$). After that, the samples were dried for 15 min in N_2-filled glovebox. For thermal stability test, the samples were annealed in N_2-filled condition at 120 °C for a given time. Then, the PNDIT-F3N-Br solution (1 mg mL^{-1} in methanol) was spin-casted onto the active layer films at 3000 rpm for 30 sec. Finally, the 120 nm of Ag electrode (CPDT-ICMe, ZY-4Cl) and 20 nm of Ca/100 nm of Al electrode ($PC_{61}BM$) were deposited by thermal evaporation in an evaporation chamber under high vacuum (~ 10^{-6} Torr) conditions. The photoactive area of the OSC devices is 0.164 cm^2, measured by OM.

OSC measurements

A McScience K201 LAB55 solar simulator and Keithley 2400 SMU were used to determine the photovoltaic performance and properties of the OSCs under AM1.5G 100 mW cm^{-2}. A McScience K3100 was used to calculate external quantum efficiency (EQE) spectra of the OSCs. A McScience K801SK302 standard cell was used to calibrate solar intensity.

Space charge-limited current (SCLC) measurements

Charge carrier mobilities of pristine and blend film were calculated by the space-charge-limited current method. ITO/zinc oxide (ZnO)/active layer/LiF/Al structure was used for electron only devices and ITO/PEDOT:PSS/active layer/Au structure was used for hole only devices. The active layers were identical to the OSC device fabrication. The Mott-Gurney equation was used to fit the measured *J-V* characteristics.

$$J_{SCLC} = \frac{9}{8}\varepsilon_0\varepsilon_r\mu(V^2L^{-3})$$

where ε_0 is free-space permittivity, ε_r is dielectric constant of the semiconductor, μ is the charge carrier mobility, V is the applied voltage and L is thickness of the active layer.

Measurements of Glass Transition Temperatures

Non-fullerene small-molecule acceptors (NFSMAs) (i.e., CPDT-ICMe, ZY-4Cl and EH-IDTBR) were prepared in tetrahydrofuran solutions with 20 mg mL^{-1}. The solution was stirred at 60 °C until being fully dissolved. Then, the solutions were spin-casted on the glass substrates with 2000 rpm. UV-vis spectroscopy was used to determine the glass transition temperature (T_g). UV-vis spectra of as-cast thin films were measured first. Then, the absorption spectra of NFSMA thin films were measured with increasing thermal annealing temperatures. Then, the temperature of the films was increased until it reached to a target temperature and

became stabilized for 5 min prior to the measurements. The same procedure was repeated with the higher annealing temperature. The transition temperature of absorption spectra was estimated as T_g. To analyze the quantitative value, the deviation metric (DM_T) method was used, which was reported by Samuel E. Root et al.[2]

$$DM_T \equiv \sum_{\lambda_{min}}^{\lambda_{max}} \left[I_{RT}(\lambda) - I_T(\lambda) \right]^2$$

where λ is the wavelength, λ_{max} and λ_{min} are the upper and lower bounds of the optical sweep, respectively, $I_{RT}(\lambda)$ and $I_T(\lambda)$ are the normalized absorption intensities of the as-cast (room temperature) and annealed films, respectively. Then, T_gs of NFSMAs were estimated at the onset point of temperature when the slope of DM_T rapidly increases and shows clear discontinuity. Finally, the processes related with measuring T_g for each sample was repeated more than 3 times to obtain the average values and standard deviations.

Supplementary Figures and Tables

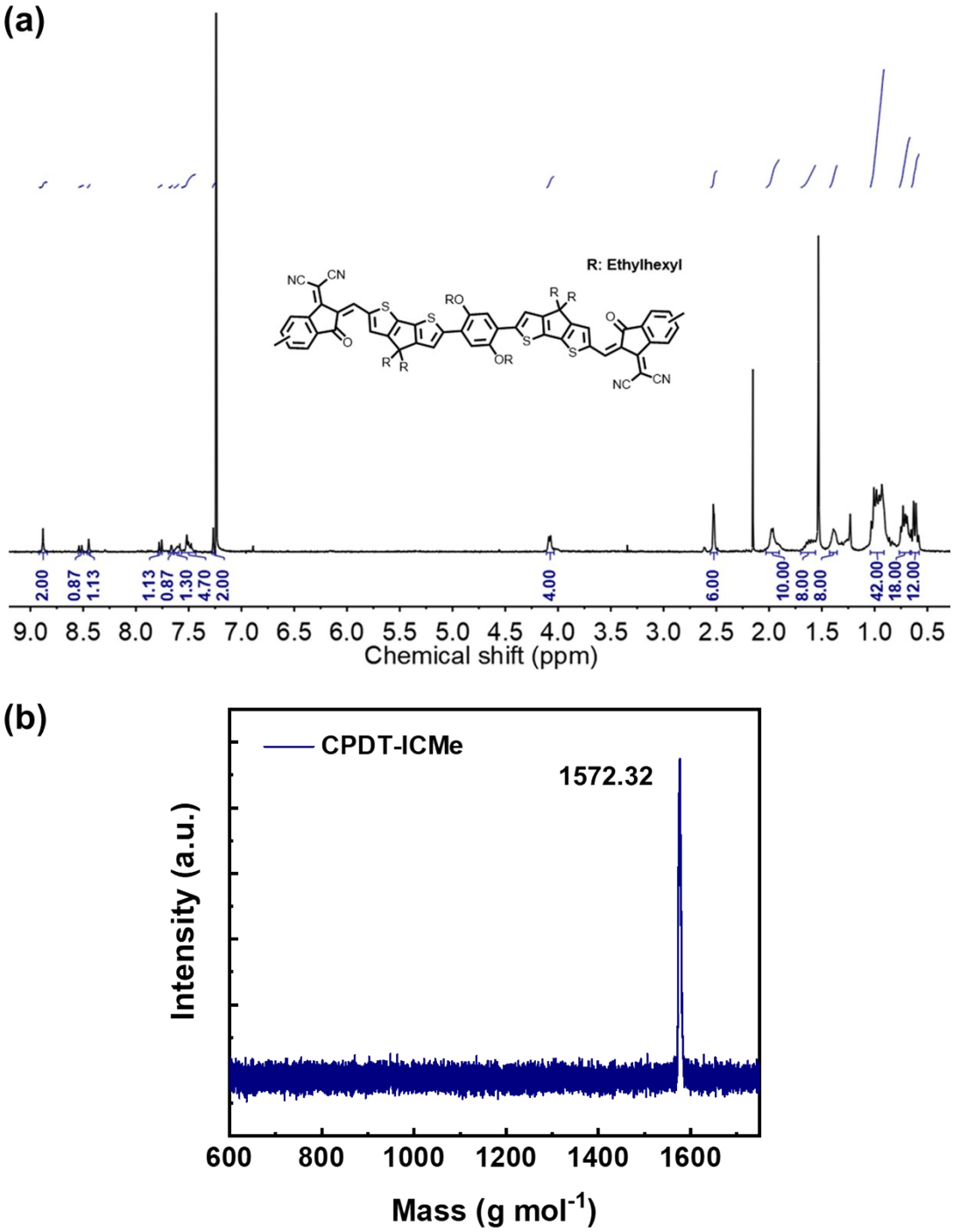

Fig. S1. (a) ^{1}H-NMR and (b) MALDI-TOF results of CPDT-ICMe

^{1}H NMR ($CDCl_3$, 300 MHz): δ_H 8.88 (s, 2H), 8.54 (d, J = 8.2 Hz, 0.87H), 8.45 (s, 1.13H), 7.78 (d, J = 7.6 Hz, 1.13H), 7.66 (s, 0.87H), 7.61 (s, 1.30H), 7.52-7.45 (m, 4.70H), 7.27(s, 2H), 4.07 (d, J = 5.2 Hz, 4H), 2.52 (s, 6H), 2.09-1.91 (m, 10H), 1.72-1.56 (m, 8H), 1.42 (s, 8H), 1.06-0.93 (m, 42H), 0.81-0.70 (m, 18H), 0.67-0.61 (m, 12H)

MS (MALDI-TOF) calcd. for $C_{100}H_{122}N_4O_4S_4$ [M^+] 1572.32, found 1572.32).

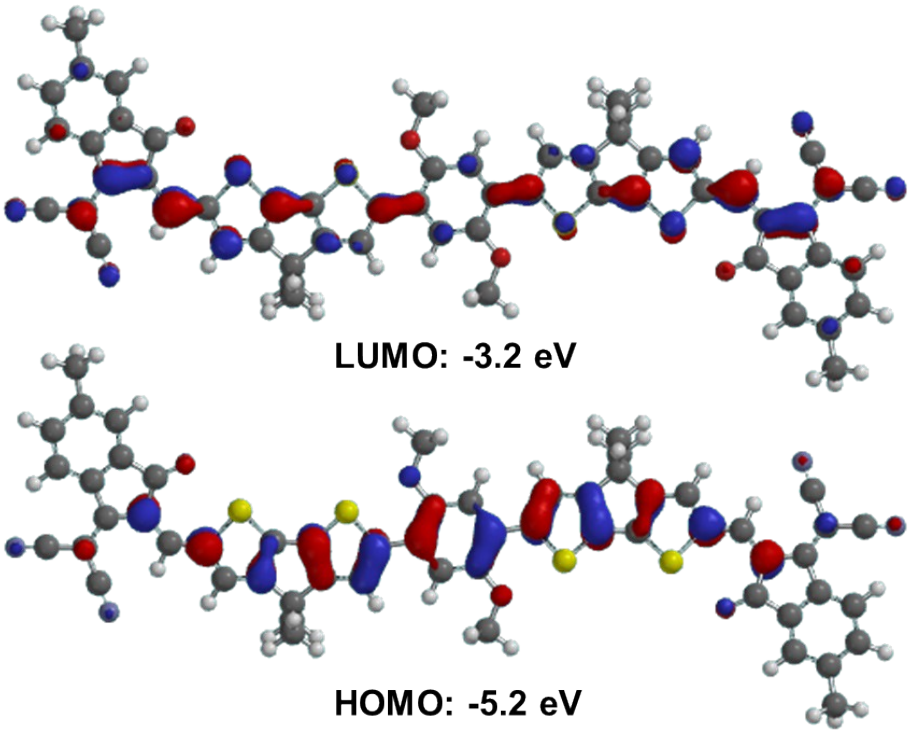

Fig. S2. Frontier molecular orbital distribution for CPDT-ICMe from density functional theory (DFT) calculation with the B3LYP functions and the 6-31G* basis set.

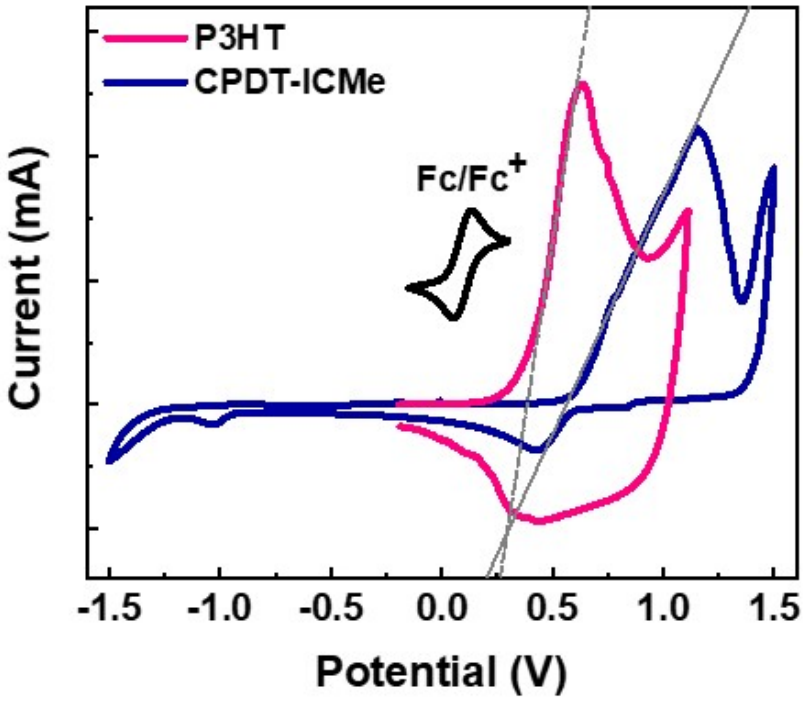

Fig. S3. CV curves of the P3HT and CPDT-ICMe.

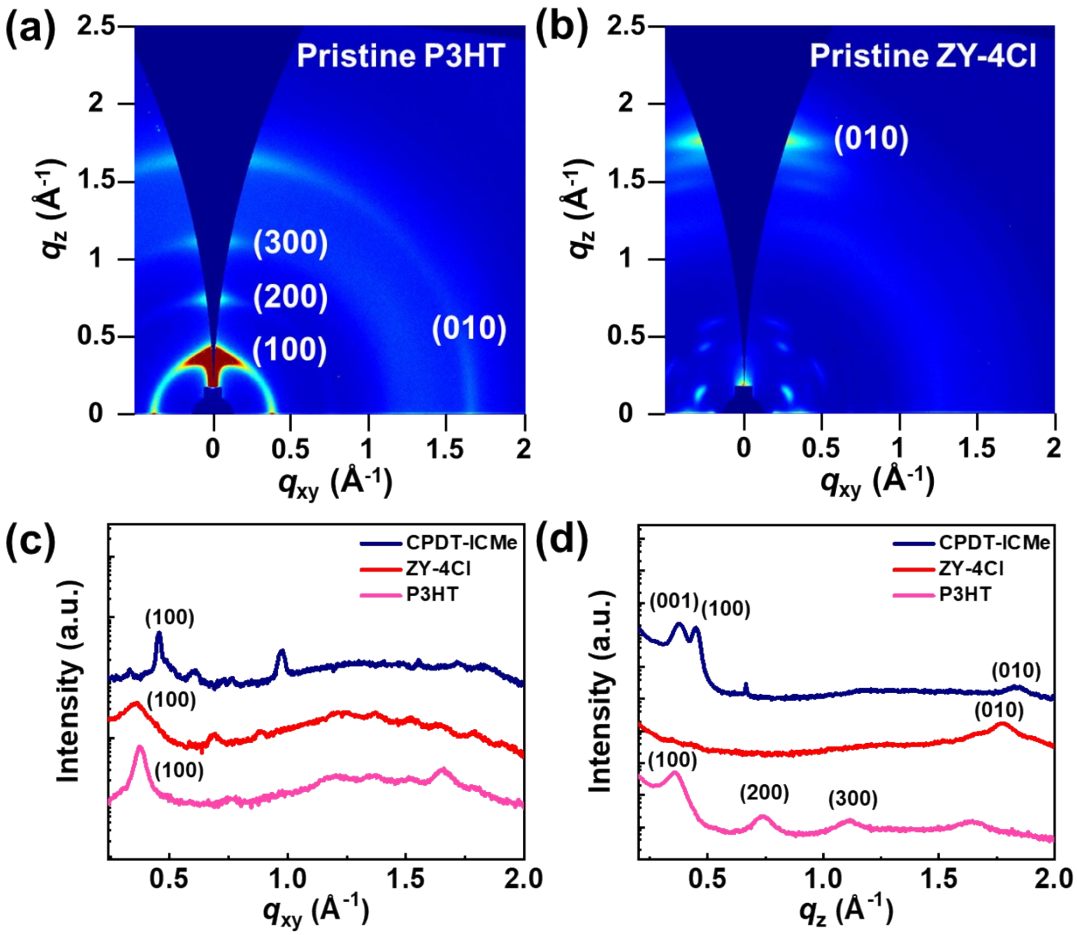

Fig. S4. 2D-GIXS images of (a) P3HT and (b) ZY-4Cl pristine films. The GIXS line-cuts of P3HT, CPDT-ICMe, and ZY-4Cl pristine films at the (c) IP and (d) OOP direction.

Table S1. The *d*-spacing values of the (100) and (010) peaks of pristine films of CPDT-ICMe, ZY-4Cl, and P3HT.

Material	Peak	*d*-spacing (Å)
CPDT-ICMe	100(IP)	13.79
	010(OOP)	3.43
ZY-4Cl	100(IP)	17.50
	010(OOP)	3.54
P3HT	100(IP)	16.71
	010(IP)	3.79
	010(OOP)	3.82

Table S2. SCLC charge mobilities of CPDT-ICMe pristine and P3HT:CPDT-ICMe blend films.

Acceptor	$\mu_{e,pristine}$[a] ($cm^2\ V^{-1}\ s^{-1}$)	$\mu_{e,blend}$[b] ($cm^2\ V^{-1}\ s^{-1}$)	$\mu_{h,blend}$[b] ($cm^2\ V^{-1}\ s^{-1}$)
CPDT-ICMe	3.07×10^{-6}	1.85×10^{-5}	8.45×10^{-5}

[a] Pristine film at as-cast condition. [b] Blend films were prepared with the same condition for the optimal OSC devices.

Table S3. Photovoltaic performances of P3HT:acceptor devices during different annealing times at 120 °C.

Acceptor	Time (hr)	$V_{oc}^{a,b}$ (V)	$J_{sc}^{a,b}$ (mA cm^{-1})	FF^{a,b}	PCE$^{a,b}_{avg}$(max)
CPDT-ICMe	0	0.76±0.01	15.36±0.22	0.63±0.01	7.36±0.12 (7.52)
	24	0.76±0.01	15.75±0.23	0.61±0.01	7.26±0.12 (7.41)
	48	0.76±0.00	15.61±0.57	0.61±0.01	7.22±0.14 (7.34)
	72	0.76±0.01	15.59±0.27	0.60±0.01	7.10±0.11 (7.23)
	100	0.75±0.01	16.30±0.17	0.60±0.00	7.25±0.17 (7.42)
ZY-4Cl	0	0.89±0.00	15.81±0.17	0.62±0.01	8.74±0.02 (8.77)
	24	0.87±0.01	15.25±0.50	0.59±0.01	7.84±0.38 (8.18)
	48	0.80±0.02	12.20±0.77	0.54±0.02	5.32±0.56 (6.16)
	72	0.73±0.05	10.96±0.72	0.47±0.01	3.75±0.38 (4.25)
	100	0.72±0.06	9.55±0.24	0.50±0.01	3.46±0.33 (3.88)
$PC_{61}BM$	0	0.57±0.00	9.30±0.05	0.64±0.01	3.37±0.08 (3.48)
	24	0.50±0.01	6.34±0.16	0.27±0.01	0.84±0.04 (0.87)
	48	0.44±0.01	5.56±0.25	0.23±0.01	0.57±0.05 (0.60)

[a] All parameters represent average values measured from more than five devices. [b] The blend films were annealed at 120 °C under inert conditions.

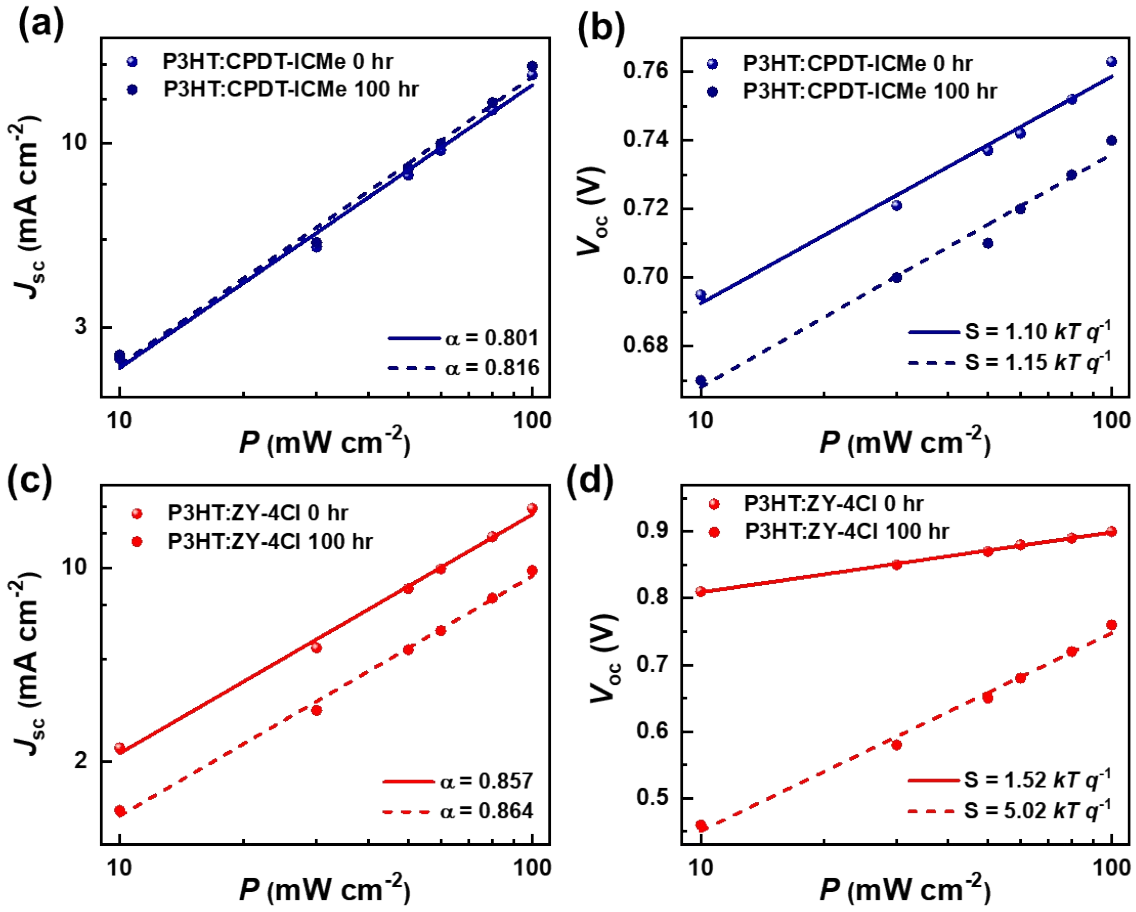

Fig. S5. The electrical properties of the blend films at 0 and 100 hr under 120 °C thermal annealing. The light intensity vs. J_{sc} and V_{oc} curves for the (a, b) P3HT:CPDT-ICMe and (c, d) P3HT:ZY-4Cl films.

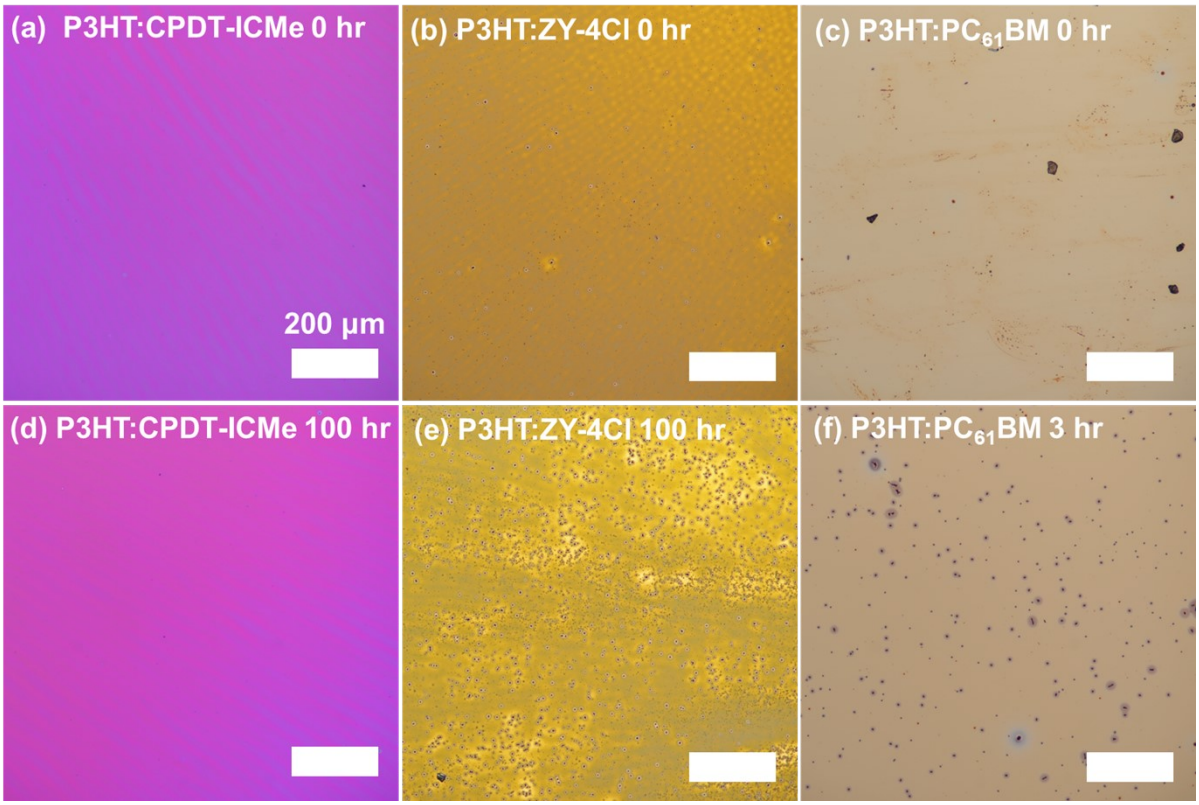

Fig. S6. OM images of different blend films at (a, b, c) 0 hr, (d, e) 100 hr, and (f) 3 hr under 120 °C thermal annealing.

.

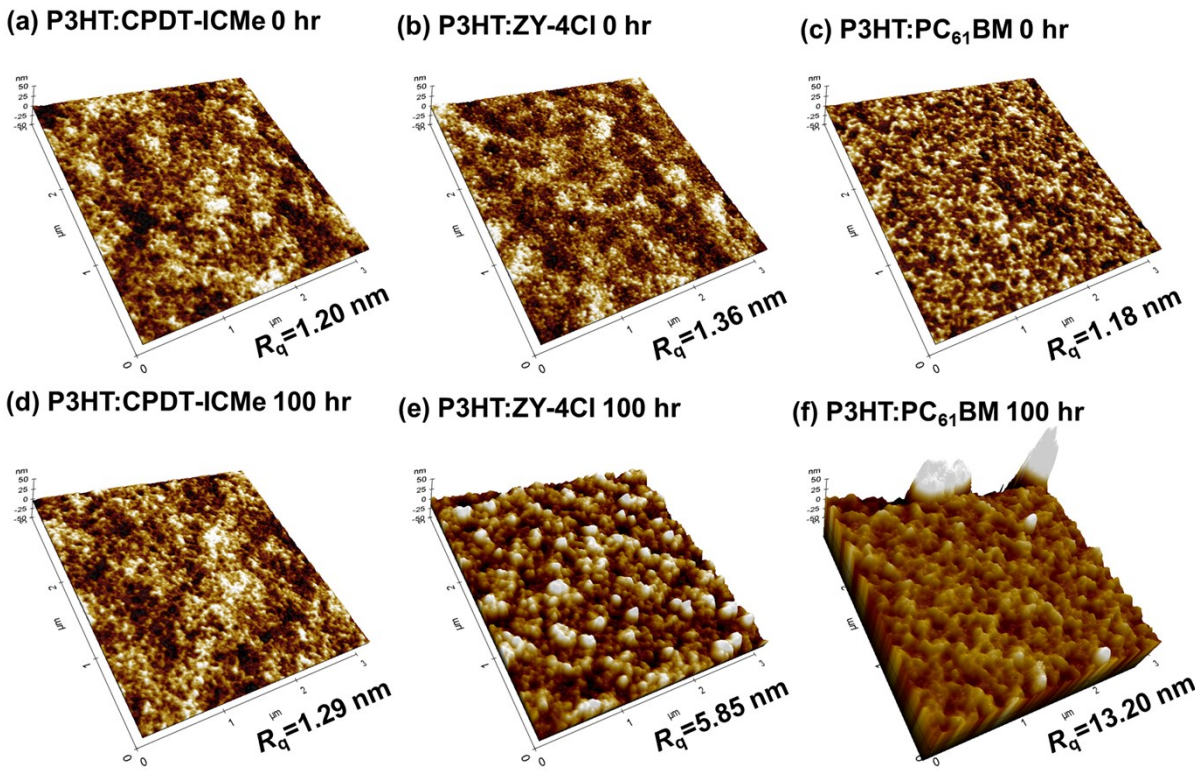

Fig. S7. AFM height images of different blend films at (a, b, c) 0 hr and (d, e, f) 100 hr under 120 °C thermal annealing.

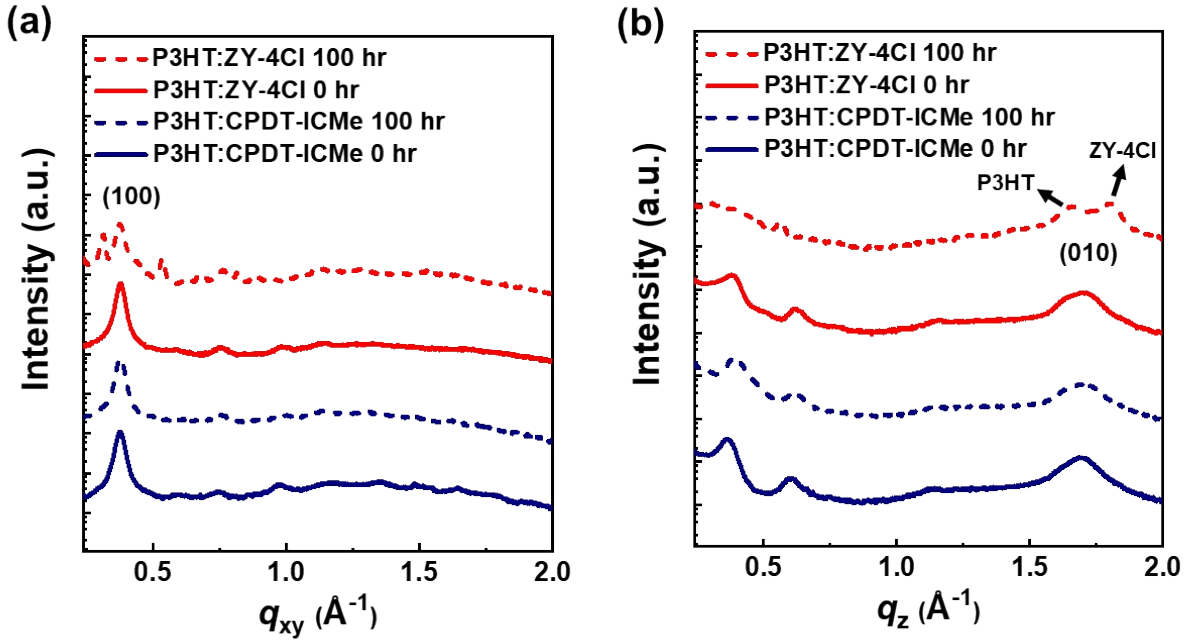

Fig. S8. (a) IP and (b) OOP line-cuts of the GIXS images of the P3HT:CPDT-ICMe and P3HT:ZY-4Cl blend films at 0 and 100 hr under 120 °C thermal annealing.

Table S4. The *d*-spacing values of (010) peak in the blend films at 0 and 100 hr under 120 °C thermal annealing.

Blend	Time (hr)	Peak	*d*-spacing (Å)
P3HT:CPDT-ICMe	0	010(OOP)	3.70
	100	010(OOP)	3.70
P3HT:ZY-4Cl	0	010(OOP)	3.70
	100	010(OOP)	3.53, 3.81

Table S5. Relative domain purities estimated from the RSoXS profiles of P3HT:CPDT-ICMe and P3HT:ZY-4Cl blend films at 0 and 100 hr under 120°C thermal annealing.

Acceptor	Time (hr)	*d*-spacing (nm)	Relative domain purity
CPDT-ICMe	0	69.8	0.49
	100	69.8	0.51
ZY-4Cl	0	-	0.43
	100	209.4	1.00

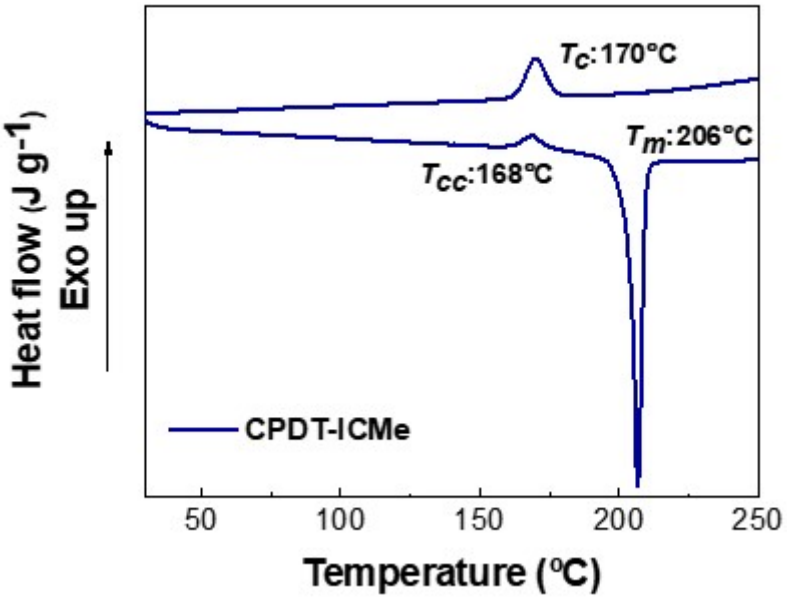

Fig. S9. DSC thermogram of CPDT-ICMe for the 1st heating and cooling cycles. The samples are collected from the solution-processed films on the glass substrate.

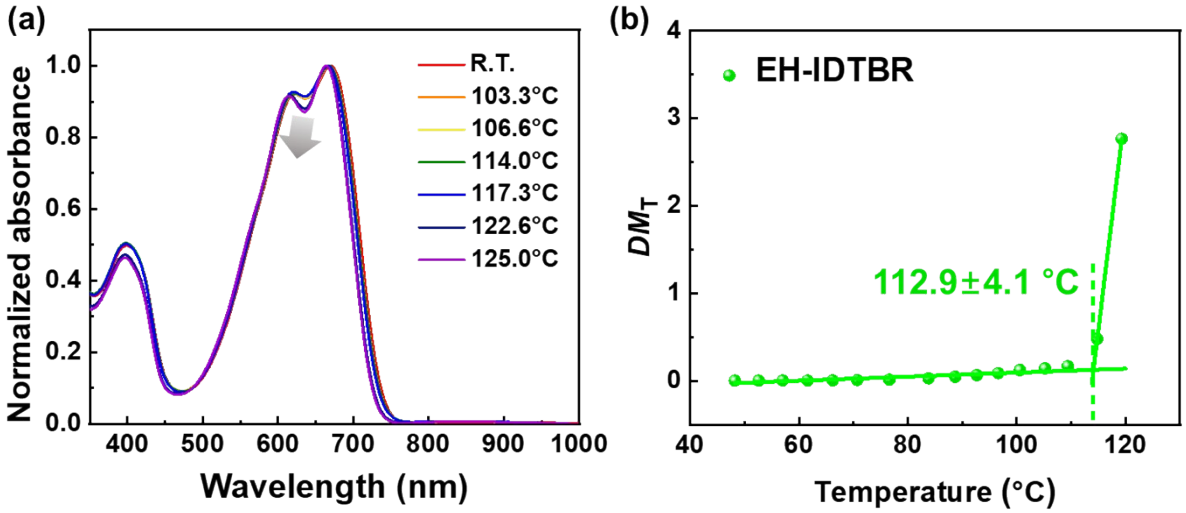

Fig. S10. (a) Normalized UV–vis absorption spectra at different temperatures and (b) UV-vis DM_T results of EH-IDTBR thin films.

References

1. T. E. Kang, H. H. Cho, H. J. Kim, W. Lee, H. Kang and B. J. Kim, *Macromolecules*, 2013, **46**, 6806-6813.
2. S. E. Root, M. A. Alkhadra, D. Rodriquez, A. D. Printz and D. J. Lipomi, *Chem. Mater.*, 2017, **29**, 2646-2654.